Contents list available at IJRED website

Int. Journal of Renewable Energy Development (IJRED)

Journal homepage: http://ejournal.undip.ac.id/index.php/ijred

Optimum Sizing Algorithm for An Off-Grid Plant Considering Renewable Potentials and Load Profile

Nabiha Brahmi*, Sana Charfi and Maher Chaabene

Faculté des sciences de Gafsa, Compus universitaire sidi Ahmed zarroug, 2112 Gafsa, Tunisia University of Sfax, Tunisia

ABSTRACT. The energy demand in remote area cannot be satisfied unless renewable energy based plants are locally installed. In order to be efficient, such projects should be sized on the basis of maximizing the renewable energies exploitation and meeting the consumer needs. The aim of this work is to provide an algorithm-based calculation of the optimum sizing of a standalone hybrid plant composed of a wind generator, a photovoltaic panel, a lead acid-battery bank, and a water tank. The strategy consists of evaluating the renewable potentials (solar and wind). Obtained results are entered as inputs to established generators models in order to estimate the renewable generations. The developed optimal sizing algorithm which is based on iterative approach, computes plant components sizes for which load profile meet estimated renewable generations. The approach validation is conducted for A PV/Wind/Battery based farm located in Sfax, Tunisia. Obtained results proved that the energetic need is covered and only about 4% of the generated energy is not used. Also a cost investigation confirmed that the plant becomes profitable ten years after installation.

Keywords: Optimization, sizing algorithm, hybrid system, load profile, energy balance

Article History: Received June 24th 2017; Received in revised form September 26th 2017; Accepted Sept 30th 2017; Available online
Citation: Brahmi, N., Charfi, S., and Chaabene, M. (2017) Optimum Sizing Algorithm for an off grid plant considering renewable potentials and load profile. Int. Journal of Renewable Energy Development, 6(3), 213-224.
https://doi.org/10.14710/ijred.6.3.213-224

1. Introduction

Following the technological revolution that has marked the past century, fuel prices have raised. In addition, fuel will break off in the following few decades. Thus, the world has moved towards the use of renewable energy in its various forms to cover its needs and fill gaps in traditional sources (Glasnovic et al. 2011; Chowdhury et al. 2011). Researches on renewable energies have been strongly developed over recent years. Plants become decentralized to consume locally the generated energy and avoid energy transport. Considered as autonomous systems, these plants are usually installed in remote area (Cano et al. 2014). Furthermore, plants are designed to gather many renewable energy forms: wind, photovoltaic (PV), etc. The design takes into account the site potential and the energy need. Hence, the plant must be characterized then its components must be sized on the basis of the renewable potentials assessment and consumer need.

In literature, many techniques have been developed for sizing optimization. Gupta et al.(2007) carried out the development of a computational model for optimal sizing of a hybrid energy system. Renewable potentials are evaluated through mathematical models, merging real meteorological data and load profile. The sizing evaluation is done in terms of loss of power supply probability (Gupta et al. 2007). Also, the main attribute of a hybrid system is the capability to satisfy energetic plant needs. The over energy production is stored in order to be used while deficit circumstances (Silva et al. 2011). A hybrid system optimum sizing using discrete version of harmony search was published (Maleki et al. 2016). The algorithm is easy to implement and can escape from local optima. Likewise, an efficient Artificial Bee Swarm Optimization (ABSO) algorithm is proposed to minimize the objective function (Maleki et al. 2014). The total annual cost is computed then the maximum allowable loss of power supply probability (LPSPmax) is taken into account to improve the system effectiveness. Similarly, a sizing optimization approach of stand-alone hybrid wind/PV/diesel energy has been presented by minimizing the cost function of the system that offers the system energy availability (Belfkira et al. 2011). Equally, Diaf et al.(2007) fixed the optimal number and type of hybrid system units in terms of

* Corresponding author: brahminabiha@gmail.com

technical and economical concepts: the loss of power supply probability and the levelised cost of energy (Diaf et al. 2007). Other researchers developed various tools to solve the sizing adequacy such as Genetic Algorithms (Tina et al. 2006), probabilistic approach (Grimsmo et al. 2005; Zhou et al. 2010), iterative technique (Musgrove 1988), dynamic programming (Bashir et al. 2012), and Monte Carlo approach (Yang et al. 2002). Hence, in order to ensure a defined autonomy for the system, different case studies are performed. Likewise, using wind and solar measurements from a meteorological station installed in Ekren et al.(2009) investigated the performance of PV/Wind hybrid system under to distinct load demand profiles (Ekren et al. 2009). Kazem and al. (2013) proposed a novel sizing strategy to increase the system reliability and reduce energy cost for a stand-alone PV system as well as tilt angle for remote areas in Sohar, Oman (Kazem et al. 2013). Kaldellis et al. (2012) estimated the size of a combined PV / wind based hybrid system, located in the Greek territory, to provide the energy demand of typical remote consumers under the criterion of minimum first installation cost (Kaldellis et al. 2012).

This paper puts forward a concrete and pragmatic sizing optimization of a hybrid stand-alone PV/wind/battery plant which considers the energetic characterization of the site and the consumer need.

2. System configuration and modeling

2.1. System configuration

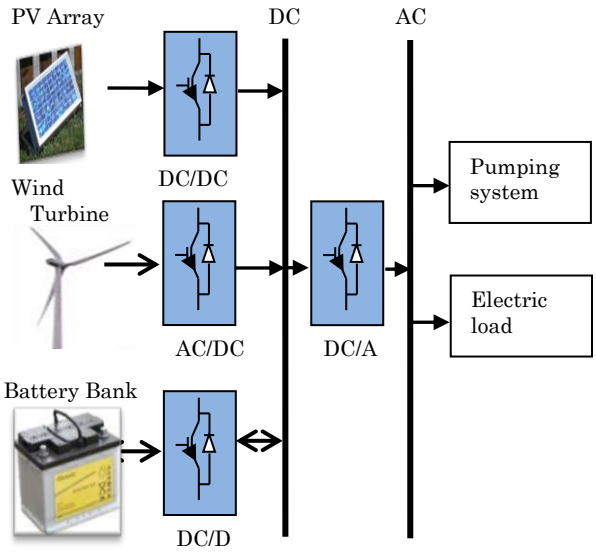

Fig. 1. Block diagram of a hybrid PV/Wind generators and storage system

A hybrid renewable energy grid is composed of Direct Current (DC) bus that gathers over inverters a photovoltaic panel and a wind turbine. Since renewable energy sources are intermittent, a storage system is included so as to store the unconsumed generated energy and to supply the load in case of energy deficiency. Thus, the considered plant becomes autonomous (Fig. 1).

The work aims to characterize the plant components on the basis of the potentials assessment and the energetic needs. The PV array delivers a DC current function of solar irradiance and ambient temperature. A boost converter is used to increase the output voltage. As for the Wind Energy Conversion System (WECS), it is based on a Permanent Magnetic Synchronous Generator (PMSG) which is coupled to the DC bus via a rectifier. Finally, a battery is coupled to a bidirectional converter in order to store over generated energy and supply the plant in case of energy deficiency. Since loads are supplied by alternative current, a DC/AC inverter is added to the installation.

The system sizing is structured around three steps: the estimation of renewable energy potentials, the evaluation of renewable generations on the basis of energy sources models and the load profile characterization (Fig. 2).

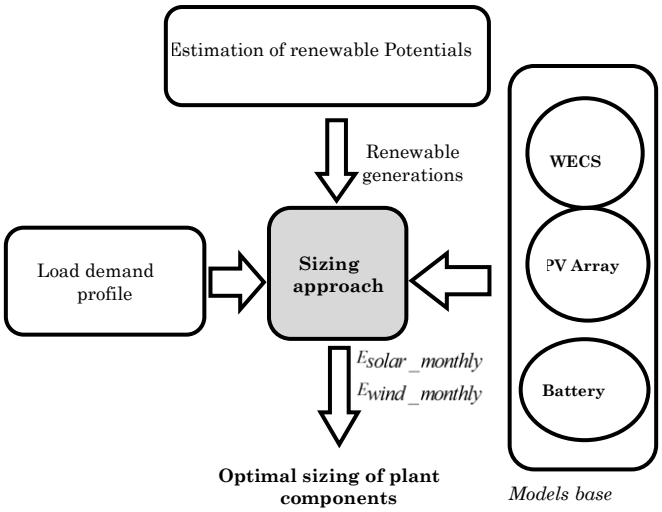

Fig. 2. Sizing Approach characterization

2.2. Estimation of renewable energy potentials

2.2.1. Solar potential

The monthly average of solar energy is given by:

$$E_{solar\_monthly} = \frac{(30 \times G_d)}{1000} \ (KWh / month / m^2) \quad (1)$$

Where G_d is the daily global solar radiation provided by the Tunisian National Meteorological Institute (INM).

2.2.2. Wind potential

The monthly wind energy is expressed by:

$$E_{wind\_monthly} = \frac{(24 \times 30 \times P_{wind})}{1000} \ (KWh / month / m^2) \quad (2)$$

$$P_{wind} = \frac{1}{2}\rho_{air}(1+3I^2)\times c^3\Gamma(1+\frac{3}{k}) \quad (3)$$

The turbulence intensity I characterizes the wind variability in high frequency (order of second). k and c are the two parameters of the Weibull distribution. This distribution is the most famous approach that permits to establish the wind potential assessment (Brahmi et al. 2012). The probability density function of the wind speed is defined as:

$$f(v) = \frac{k}{c}\left(\frac{v}{c}\right)^{k-1} e^{\left(-(\frac{v}{c})^k\right)} \quad (4)$$

The corresponding cumulative distribution function is given by:

$$F(v) = e^{\left(-(\frac{v}{c})^k\right)} \quad (5)$$

Many methods are used in the determination of k and c: the Least Squares Method (LSQ) (Seguro, et al. 2000), the Maximum Likelihood Method (MLM) (Yang et a.. 2003), and the Modified Maximum Likelihood Method (MMLM) (Arbaoui 2006). These methods are compiled to compute k and c using the available monthly meteorological database. In previous work Brahmi et al. (2012), the parameters k and c were determined by the MMLM method. The wind potential is calculated on the basis of the Weibull distribution using its shape and scales parameters. The characteristic speeds are expressed as follows:

$$v_m = c\Gamma(1+\frac{1}{k}) \quad (6)$$

$$v_E = c\Gamma(1+\frac{2}{k})^{\frac{1}{k}} \quad (7)$$

$$v_F = c\Gamma(1-\frac{1}{k})^{\frac{1}{k}} \quad (8)$$

WhereΓ is the defined gamma function, for any real number x positive not null, by:

$$\Gamma(x) = \int_0^\infty t^{x-1}e^{-t}dt$$

The Weibull distribution I has the advantage of giving an excellent recovery of the experimental database and of envisaging the wind power for various heights (Parket al 2004). Indeed, knowing the mean speed (V_a) at height Z_a, the mean speed $V_m(z)$ at the height z is given as:

$$v_m(z) = v_a\left(\frac{z}{z_a}\right)^{\alpha};\ a=\frac{x\text{-}0.088log(v_a)}{1\text{-}0.0881log(\frac{z_a}{10})} \quad (9)$$

2.3. System modeling

2.3.1. PV system model

The common empirical model of an equivalent circuit photovoltaic cell is based on a one diode (Fig. 3).

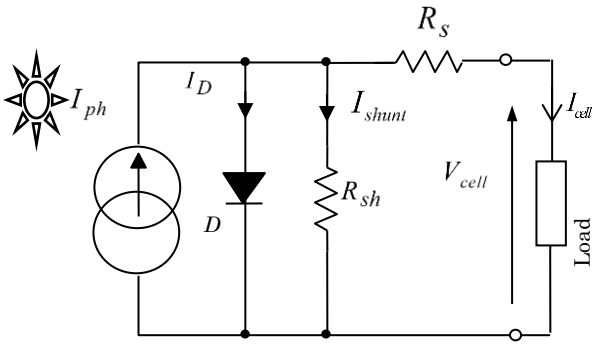

Fig. 3. Electrical model of a solar cell

The output current of the PV cell can be described as (Gokcek et al.2007):

$$I_{cell} = I_{ph} - I_d - I_{shunt} \quad (10)$$

The light-generated current of the PV cell I_{ph} depends linearly on the solar irradiance G and the cell temperature Taccording to the following equation:

$$I_{ph} = (I_{pv\_stc} + k_1(T - T_{ref}))\frac{G}{G_n} \quad (11)$$

$$I_{shunt} = \frac{V_{cell} + R_s I_{cell}}{R_p} \quad (12)$$

$$I_d = I_o[\exp(\frac{V_{cell} + R_s I_{cell}}{aV_t}) - 1] \quad (13)$$

Where

$$I_o = I_{o,n}\left(\frac{T_n}{T}\right)^3 \exp[\frac{qE_g}{ak}(\frac{1}{T_n} - \frac{1}{T})]$$

$$I_{o,n} = \frac{I_{sc,n} + K_1\Delta T}{\exp(\frac{V_{oc,n} + K_v\Delta T}{aV_{t,n}}) - 1}$$

The PV array is composed of Ns serial PV cells connected in Np parallel branches. The whole generated current $I_{pv}$is given by:

$$I_{pv} = Np\left(I_{pv-stc} + K_1\left(T - T_{ref}\right)\frac{G}{G_n}\right) - Np\left(I_o\left(exp\left(\frac{V_{pv} + R_s I_{pv}\left(\frac{Ns}{Np}\right)}{aNsV_t}\right) - 1\right)\right) - \left(\frac{V_{pv} + R_s I_{pv}\left(\frac{Ns}{Np}\right)}{R_p\left(\frac{Ns}{Np}\right)}\right) \quad (14)$$

The photovoltaic generated power is:

$$P_{pv} = I_{pv} \times V_{pv} \quad (15)$$

2.3.2. Wind Generator

The wind generator is composed of a wind turbine coupled to Permanent Magnetic Synchronous Generator (PMSG) (Fig.4).

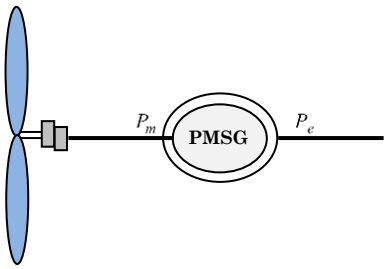

Fig. 4. Wind generator

The output power of the generator is determined as follows (Lin et al. 2010):

$$P_e = P_m 0.87 P_n^{0.014} \quad (16)$$

Where P_n is the nominal power of the PMSG and P_m represents the mechanical power of the turbine. It is expressed by the following equation (Melício et al. 2011):

$$P_m = \frac{\rho.\pi.R^2.C_p.v^2}{2\Omega_m} \quad (17)$$

$$\Omega_m = G_{gear}\Omega_t \quad (18)$$

$C_m$is the power coefficient defining the aerodynamic efficiency of the wind turbine rotor. It depends on the wind velocity and the tip speed ratio λ. According to the Betz law, the power coefficient C_p can never exceed 0.593, it is expressed by (Slootweg et al 2003):

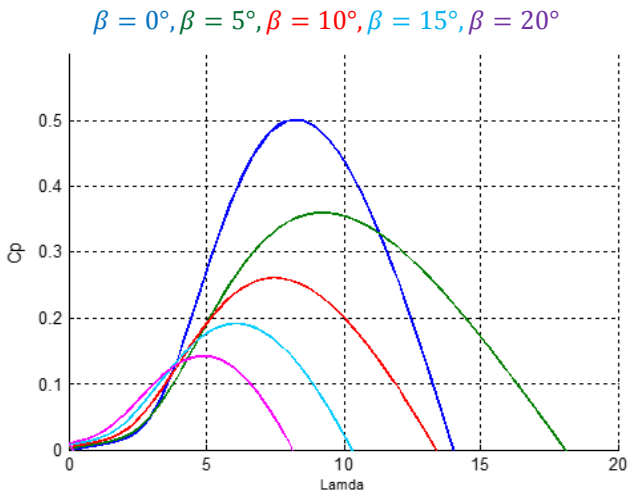

Fig. 5. Wind power coefficient variation function of the pitch angle

$$C_p(\lambda,\beta) = 0{,}73\left(\frac{151}{\lambda\iota} - 0{,}58\beta - 0{,}002\beta^{2{,}14} - 13.2\right)e^{\left(\frac{-18{,}4}{\lambda i}\right)} \quad (19)$$

Where $\lambda = \frac{\Omega R}{v}$ and $\lambda_i = \frac{1}{\frac{1}{\lambda - 0.02\beta} - \frac{0.003}{\beta^3+1}}$.

Figure 5 shows the variation of the power coefficient versus the tip speed ratio for different pitch angle $C_p(\lambda,\beta)$. It reaches a maximum value of 0.5 for an optimal λ of 8.2 and a null pitch angle.

2.4. Cost assessment

Eq. 20 gives the calculation formula of the global plant cost:

$$C_{plant} = C_i + C_m + C_r \quad (20)$$

Where C_i: initial cost, C_m: maintenance cost, C_r: replacing cost

2.4.1. Initial cost

The initial cost function is expressed by Belmilin et al. (2014):

$$C_i = P_w \times C_w + P_{pv} \times C_{pv} + N_{bat} \times C_{bat} + S_{inv} \times C_{inv} + P_{chop} \times C_{chop} \quad (21)$$

Where C_{i_w}: initial cost of the wind system, C_{i_pv}: initial cost of the photovoltaic system, C_{i_bat}: initial cost of the storage system, C_{i_chop}: initial cost of the inverter, S_{inv}: apparent power of the inverters.

2.4.2. Maintenance cost

In the developed software a percentage of the initial cost for each compound is given for a period of a year (Belmilin et al. 2014).

$$C_m = N_w \times C_w \times m_w + N_{pv} \times C_{pv} \times m_{pv} + N_{bat} \times C_{bat} \times m_{bat} + S_{inv} \times C_{inv} \times m_{inv} + P_{chop} \times C_{chop} \times m_{chap} \quad (22)$$

2.4.3. Compounds replacing cost

The Compounds replacing cost is evaluated, specially, using the lifetimes of different components (Belmilin et al. 2014).

$$C_m = N_w \times C_w \times \frac{(lf_{sys} - lf_w)}{lf_w} + N_{pv} \times C_{pv} \times \frac{(lf_{sys} - lf_{pv})}{lf_{pv}} + N_{bat} \times C_{bat} \times \frac{(lf_{sys} - lf_{bat})}{lf_{bat}} + S_{inv} \times C_{inv} \times \frac{(lf_{sys} - lf_{inv})}{lf_{inv}} + P_{chop} \times C_{chop} \times \frac{(lf_{sys} - lf_{chop})}{lf_{chop}} \quad (23)$$

Where

N_w : number of wind turbines installed

N_{pv} : number of PV modules installed

N_{bat} : number of batteries installed

$lf_{sys}, lf_{pv}, P_{pv}, lf_w, lf_{bat}, lf_{chop}, lf_{inv}$ are respectively the

life-time of the whole system, photovoltaic system, the wind system, the batteries, the chopper and the inverter.

3. Sizing Algorithm

The sizing algorithm is developed in order to ensure an autonomous system and to meet the established energy constraints. The algorithm inputs are the estimated available renewable energies, the load profile and the generators models (Figure 6). The algorithm provides the photovoltaic panel surface, the surface of wind turbine blades, the tank volume and the battery capacity. The algorithm is composed of three steps:

Step I: An ANN estimation of the photovoltaic potential implication coefficient α_{pv} (the ratio of solar and wind potentials). This coefficient depends on the geographical characteristics of the sites and on the ratio of 1kW prices produced by each type of energy.

Step II: Calculation of the initial surfaces of the PV and wind generators blades using the least squares method by ensuring the satisfaction of the yearly energy need by renewable generation:

$$\sum_{i=1}^{12} E_{renewable}(i) - \sum_{i=1}^{12} Need(i) = 0 \quad (24)$$

Step III: Adjust the surfaces of PV and wind generator blades by iterative computing according to the monthly energy gap value(W_{Gap}) which is the difference between the generated and consumed energies. After convergence, the battery capacity is consequently calculated. Then the tank volume is computed on the basis of all previous sizes results.

A case study of an agriculture farm supplied by a PV/Wind/Battery system is considered. Fig. 6 shows the sizing algorithm. It computes the optimum sizes of the considered farm components: the surface of the wind generator blades, the PV array surface, the tank volume, and the battery capacity. The algorithm should ensure the load energy need throughout the year by maximizing the use of renewable energies (Brahmi et al. 2012).

3.1. Determination of photovoltaic implication coefficient

The ANN controller is used to estimate the optimum photovoltaic implication coefficient for a given solar and wind potentials. The architecture of the adopted Neural Network is composed of three layers (Fig. 7). The input layer contains two neurons as it disposes of two inputs (solar potential and wind potential: P_{wind} , P_{pv}). The hidden layer includes five neurons, this number is fixed following the execution of empirical rules which start with a high number of neurons and eliminate the unnecessary ones on condition to reach network stability and output accuracy. The output layer contains one neuron that provides the optimum α_{pv}.

The activation function of neurons is defined by the hyperbolic tangent function (Haykin, 1998):

$$Y=f(U)=W_0\times tanh(W_1\times U+b_1)+b_0 \quad (25)$$

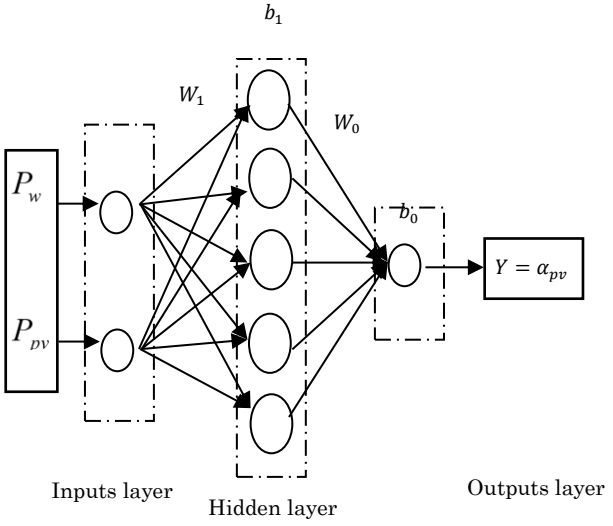

Fig. 7. Architecture of the neural network to estimate α_{pv} .

The model is based on multi-layer perception(MLP) feed-forward architecture, where Y is the outputs neural network given by the optimum photovoltaic implication coefficient, U is a column vector including the monthly mean per m^2 of solar and wind potentials. Also, the expert data base for learning and training is built according to Eq. 26:

$$Needs = \alpha_{pv}\hat{S}_{PPV}E_{pv} + (1-\alpha_{pv})\hat{S}_{wind}E_{wind} \quad (26)$$

Where

$$\alpha_{pv} = \alpha\delta \qquad \alpha = \frac{P_w(W/m^2)}{P_{pv}(W/m^2)} \qquad \delta = \frac{C_w}{C_{pv}}$$

C_w, C_{pv} are respectively the prices of 1 W produced by each generator (wind and photovoltaic), α_{pv}: Photovoltaic implication coefficient (without unit), α: factor indicating the proportionality of the two renewable potentials: photovoltaic and wind (without unit), δ: the ratio of generation costs ofwind and photovoltaicenergies (without unit).

Figure 8 shows the algorithm that determine the optimum implication coefficient α_{op}. Fist the maximum number of PV modules Npv_{max} is calculated on the basis of the estimated solar and wind potentials. Then, the number of PV modules N_{pv} is calculated thanks to an iterative loop starting with $N_{pv} = 1$ until $N_{pv} = Npv_{max}$. For each iteration, the number of wind generator is determined in order to satisfy the load. Consequently, the whole renewable generation is established $E_{renewable}(i)$ which yields to the calculation of the relative implication coefficient α_{pv}.

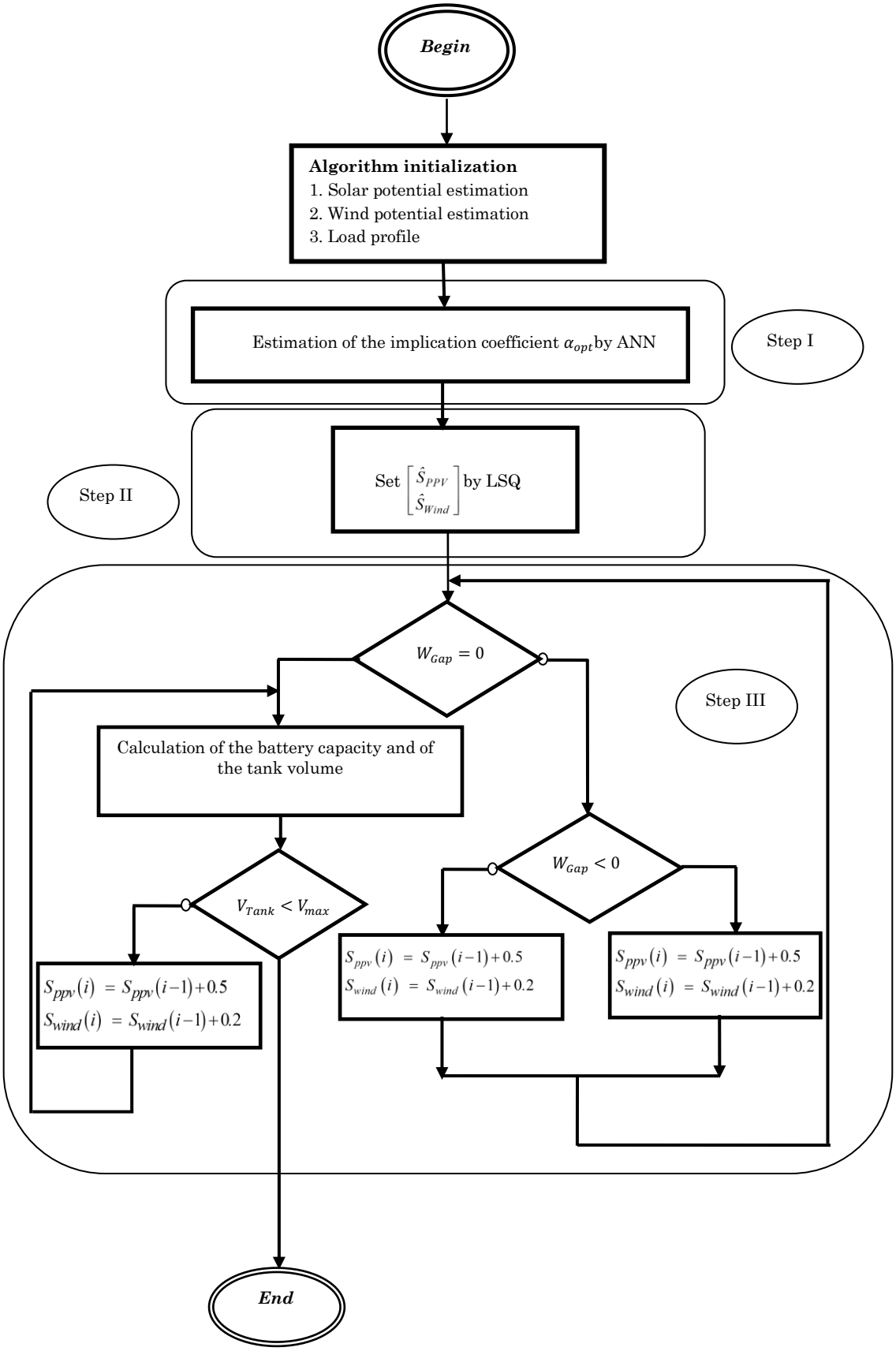

Fig. 6. Sizing algorithm

The $E_{renewable}(i)$ is then plotted function of α_{pv} and the month. The optimum value of $\alpha_{pv}(\alpha_{opt})$ is deduced on the basis of offering a yearly lost energy equal to zero $E_{renewable} = Need$

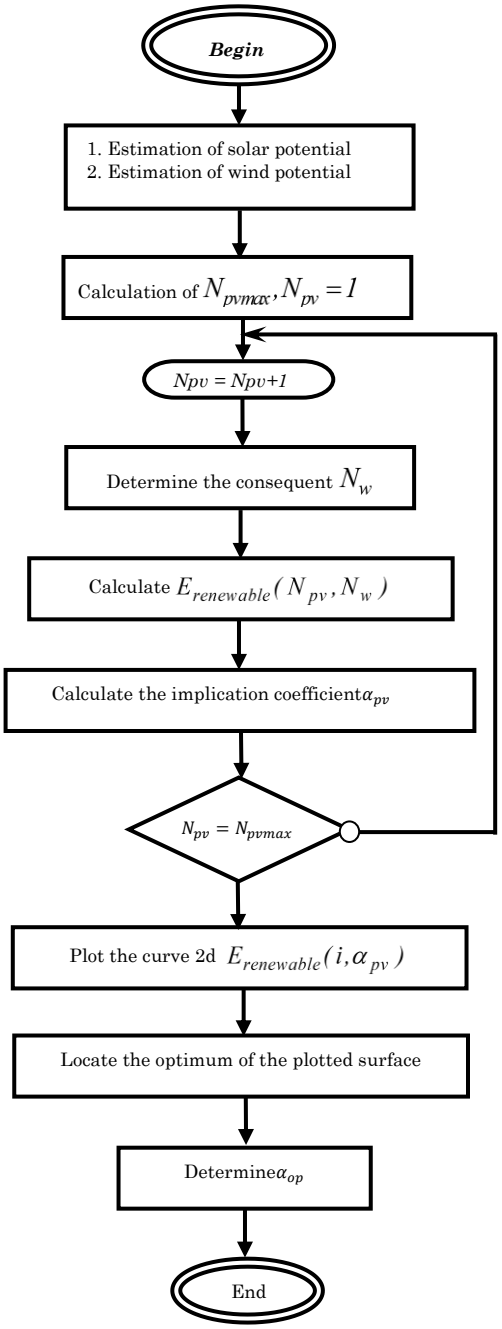

Fig. 8. Flowchart of determination of α_{op},

3.2. LSQ based estimation

The values of $\widehat{S_{PPV}}$ and $\widehat{S_{wind}}$ are estimated using the *LSQ* method applied to measurements database vectors *X*, *Y* and *Z* are composed respectively of X_I,Y_I, and $Z_I$monthly measures, by considering:

$$Z = aX + bY \tag{27}$$

Where

$$X = \begin{pmatrix} E_{m^2\_PPV\_January} \\ . \\ . \\ . \\ E_{m^2\_PPV\_December} \end{pmatrix}, \quad Y = \begin{pmatrix} E_{m^2\_wind\_January} \\ . \\ . \\ . \\ E_{m^2\_wind\_December} \end{pmatrix},$$

$$Z = \begin{pmatrix} Need\_January \\ . \\ . \\ . \\ Need\_December \end{pmatrix}, \quad H = \begin{pmatrix} E_{m^2\_PPV\_January} & E_{m^2\_wind\_January} \\ . & . \\ . & . \\ . & . \\ E_{m^2\_PPV\_December} & E_{m^2\_wind\_December} \end{pmatrix},$$

$$\varepsilon = \begin{pmatrix} \varepsilon_{January} \\ . \\ . \\ . \\ \varepsilon_{December} \end{pmatrix}, \quad \hat{\theta} = \begin{bmatrix} \hat{S}_{PPV} \\ \hat{S}_{wind} \end{bmatrix}$$

Where ε is the white noise vector. The estimated value of $\hat{\theta}$ is expressed as:

$$\hat{\theta} = (H^T H)^{-1} H^T Z \tag{28}$$

$$E_{renewable}(i) = E_{wind}(i) + E_{PPV}(i)$$
$$E_{wind}(i) = \hat{S}_{wind} E_{m^2\_wind}(i)$$
$$E_{PPV}(i) = \hat{S}_{PPV} E_{m^2\_PPV}(i)$$

Where

$E_{m^2\_PPV}$:the monthly generated photovoltaic energy per m^2 of PV panel.

$E_{m^2\_wind}$:the monthly generated wind energy per m^2 of the wind generator blades.

Also, let:

$$Needs = \begin{pmatrix} Needs\_January \\ . \\ . \\ . \\ Needs\_December \end{pmatrix}$$

$$E_{renewable} = \hat{S}_{PPV} \begin{pmatrix} E_{m^2\_PPV\_January} \\ . \\ . \\ . \\ E_{m^2\_PPV\_December} \end{pmatrix} + \hat{S}_{wind} \begin{pmatrix} E_{m^2\_wind\_January} \\ . \\ . \\ . \\ E_{m^2\_wind\_December} \end{pmatrix}$$

The quadratic error between the generated and the required energies is expressed by:

$$\varepsilon = \sqrt{\frac{1}{12}\sum_{i=1}^{12}\left(Needs(i) - E_{Renewable}(i)\right)^2} \quad (29)$$

3.3. Battery sizing

The stored energy in a battery is given by Eq. 30:

$$E_{tot} = C \times V_{bat} \quad (30)$$

The technology of the selected battery (Lead/Acid) allows 80% as Depth Of Discharge DOD_{max}=80%. The usable energy E_{usable} in the battery is expressed by Eq. 31:

$$E_{usable} = E_{tot} \times DOD_{max} = E_j \times J_{aut} \quad (31)$$

J_{aut} is the number of autonomy days.

Hence, the battery capacity is given by the Eq. 32:

$$C = \frac{Jaut.Ej}{V_{bat} DOD_{max}} \quad (32)$$

3.4. Tank sizing

The tank volume is calculated on the basis of the needed water and the excess in generated energy (Eq.33).

$$V_{tank} = \frac{3.6E_{excess}}{\rho_{water} gH} \quad (33)$$

Where E_{exess} is the excess of the monthly energy,ρ is the water density ($Kg.m^{-3}$), g is the gravity acceleration (ms^{-2}), and H is the height of rise (m).

4. Results and discussion

As previously mentioned, the main aim is to optimize the sizing of a standalone hybrid plant on the basis of renewable potentials assessment, well characteristics, and load profile. In order to validate the developed algorithm, a farm located in Sfax is considered as a case study. It is located in the South-EST of Tunisia, at latitude of $34^{\circ}43'N$ and longitude of $10^{\circ}41'E$. The approach is based on the establishment of monthly energies audit already published inBrahmi et al. 2012. A one year of a saved meteorological data base at Sfax airport station is used.

The daily wind speed at height of *12 m* is presented by Fig. 9. The wind speed varies between 1 m/s and 8.5 m/s, April is the windiest month with an average of 4 m/s.

The INM offers a data base of solar potential characteristics for 10 years. The monthly average solar irradiation is depicted in Fig. 10. It reaches its maximum from May to September.

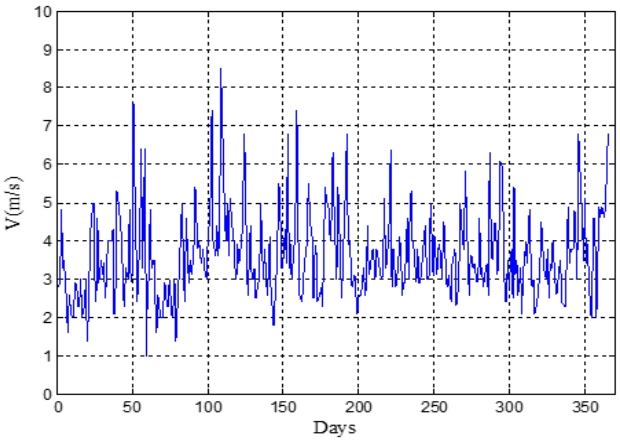

Fig.9. Measured wind speed in Sfax

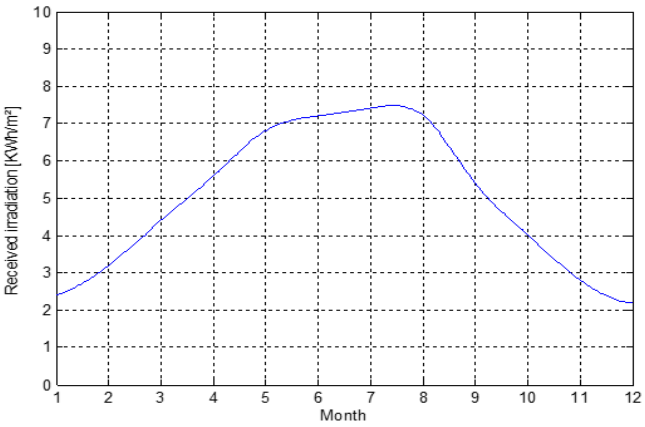

Fig. 10. Received mean monthly solar irradiation in Sfax

The curves were plotted thanks to the wind and PV models. Fig. 11 shows the curves of the monthly renewable energies generated per m^2 in Sfax, Tunisia. The wind potential in Sfax is more important than the solar potential. This is due to the availability of wind throughout the day 24h / 24h, while the sun is available only during daylight.

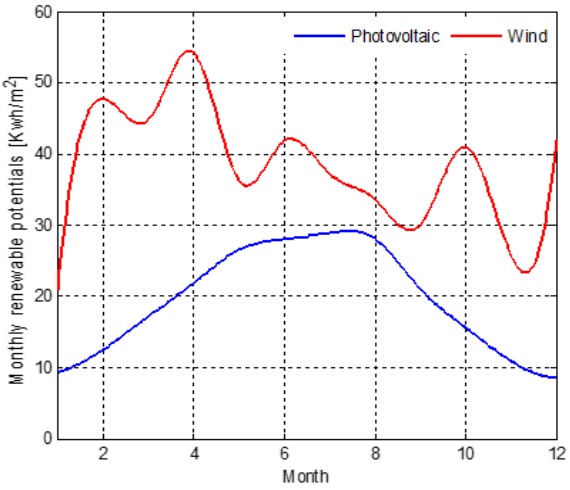

Fig. 11. Renewable potentials in Sfax

The wind speed and the solar radiation are used as inputs for the algorithm. Load profiles (in per unit of kWh) are defined for quarter-hour time-step for each day over one year. Official and floating holidays, all seasonal, weekly and daily influences (Friedl et al. 2007) are considered. Figure 12 shows a daily farm energetic consumption profiles. The curves present two peaks: at the morning (6 am) and at the evening (7 pm).

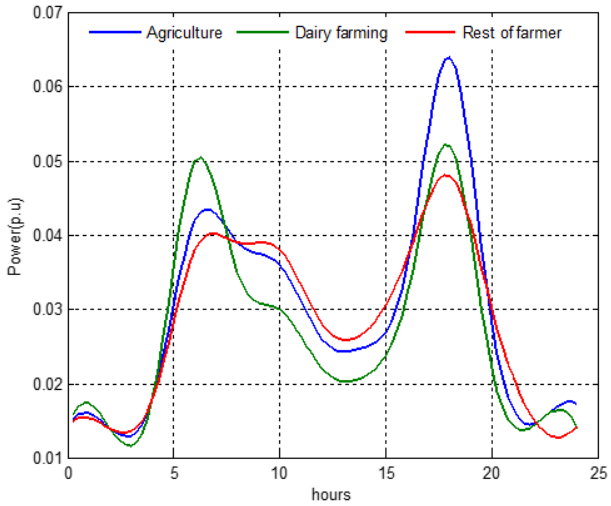

Fig. 12. Daily farm energetic consumption

Fig. 13 gathers the profiles of the loads and the renewable generations per m^2. These profiles are entered as inputs to the sizing algorithm of Figure 6.

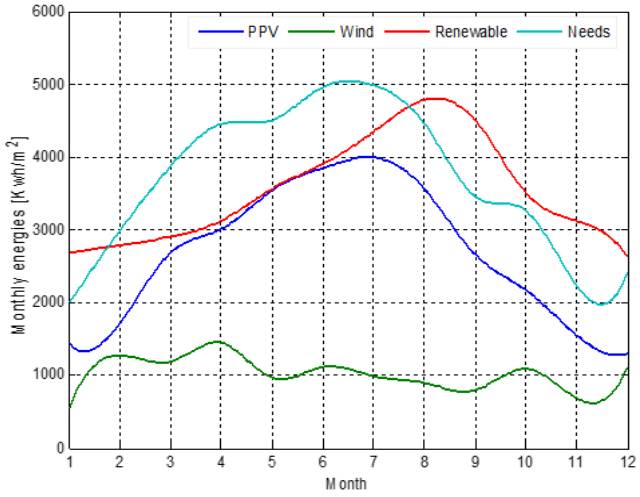

Fig. 13. The yearly generated and consumed energies

Referring to the algorithm of Figure 7, the produced renewable energy to supply a typical load of 1 KWh is plotted for each month function of the implication coefficient α_{pv} (Fig 14). Then, considering the algorithm of Figure 8. The optimum implication coefficient α_{opt} is deduced on the basis to achieve no lost energy.

Consequently, stating the obtained value of the implication coefficient α_{opt} the surfaces of PPV and turbine blades are estimated $(\widehat{S_{ppv}}, \widehat{S_{wind}})$, by using the LSQ method (§ 3.2). The computed values are:

$$\hat{S}_{ppv} = 48.10 m^2 \qquad \hat{S}_{wind} = 32.80 m^2$$

The initial estimated surfaces are entered as inputs to the sizing algorithm of Figure 6.

Following the achievement of iterations, the obtained rounded surfaces for PV panels and wind blades are:

$$S_{final\_ppv} = 136.5814 m^2$$
$$S_{final\_wind} = 26.67 m^2$$

The PPV surface is larger than the turbine wind blades surface because the wind turbine supplies energy all the time thanks to the wind conditions availability, contrary to the solar energy which is available only during daylight. Also, as well known the wind turbine efficiency is largely higher than the PPV efficiency.

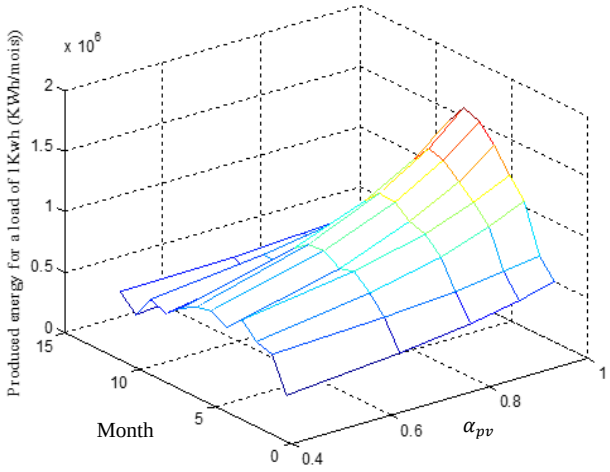

Fig. 14. Variation of produced energy in function of α_{pv} and month

The difference in the dominance of two potentials allows the calculations of the implication coefficient. For a typical load of 1 kW, Figure 15 shows the lost energy function of the implication coefficient.

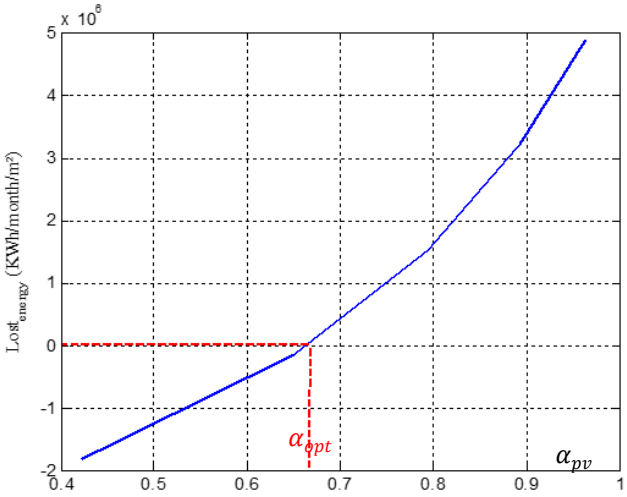

Fig. 15. Energy losses in function of α_{pv}

In order to evaluate the sizing performance, monthly need and generated energies have been analyzed by computing the energy balance over the year. Figure 16 shows the energy balance of the system during the year. An energy deficit is noticed during the 8th and the 1stmonth but this deficit is covered during the rest of the year. In fact, the yearly energy loss is evaluated at 4% using Eq.34:

$$Lost_{energy} = 100 \times \sum_{i=1}^{12} \frac{(E_{renewable}(i) - Needs(i))}{E_{renewable}(i)} \quad (34)$$

Referring to section §3.3 the battery capacity and lifetime are vital in system optimization process. By computing the luck of energy during all the year, the plant needs a battery bank of a capacity equal to *1200Ah.*Therefore, using equation 28, the obtained tank volume is $V_{tank} = 270.2296\, m^3$.

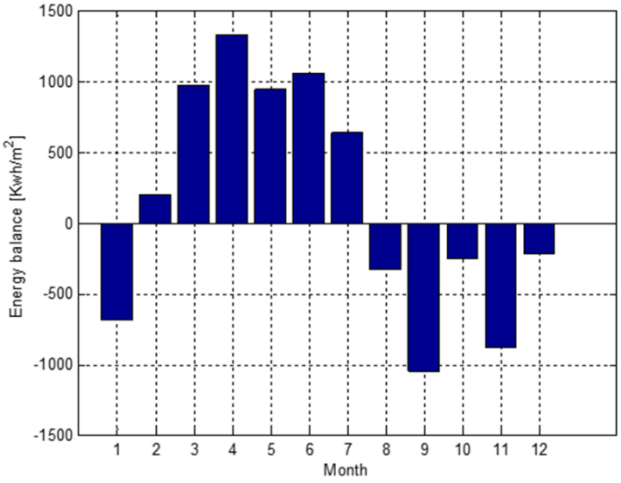

Fig. 16. Difference between monthly renewable generations and load demand.

5. Profitability

An investigation on the plant cost is carried out in order to determine the plant profitability (Belmilin al. 2014) (Eq.20). All cost parameters are described in Table 1 and Table 2

Table 1
Lifetime for the installation components (Belmilin et al. 2014)

System	Life time (Year)
Photovoltaic system lf_{pv}	20
Wind system lf_{w}	15
Inverter lf_{inv}	15
Chopper lf_{chp}	15
Storage system lf_{bat}	4

Calculations has led to:
Global cost =39137€
Initial cost= 24426 €
Maintenance cost = 299.63€
Components replacing cost=7083€

Table 2
Cost parameters for the installation components (Eftichios, et al. 2006).

Parameters	Name	Values
C_{pv} (€/ module 300Watt)	The photovoltaic module cost	180
m_{pv} (€/ module per year)	The photovoltaic module maintenance cost	2.66
C_b (€/ battery)	The battery cost	264
m_{bat} (€/ battery per year)	The maintenance cost for one battery	2.64
C_{chop} (€/chopper)	The chopper cost	200
m_{chop} (€/ chopper per year)	The maintenance cost for one chopper	2
C_{inv} (€/ inverter)	The cost of the inverter	1942
m_{inv} (€/ inverter per year)	The maintenance cost for one inverter	19.42

The different cost percentages are summarized in Fig. 17. It is obvious that the PV system cost part occupies 55% of the total installation cost. The batteries take 21% of the overall cost as they must cover the load need during night. As for the wind system, it occupies only 16% because Tunisia does not have an important wind potential.

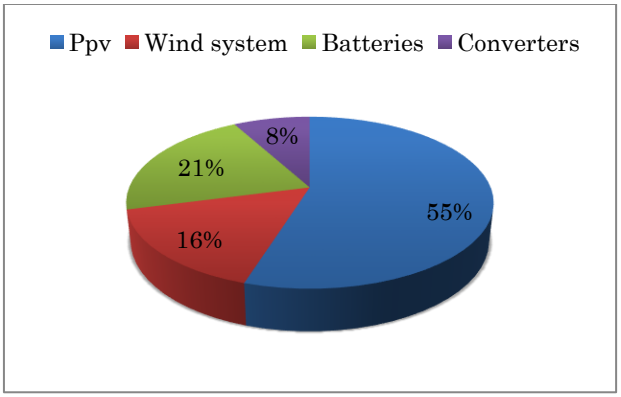

Fig. 17. Break down of annualized cost of the plant

The effectiveness of the system sizing and the economic study request a computing of the system profitability.

Referring to Tunisian prices of electricity provided in the electric power provider company (Tunisian Company of Electricity and Gas: STEG), the cost of 1 kwh is 0.167 dt and the license fees are 2.6 (dt/kW/Month) and taxes are 30% of the whole charges. As the installation need is 30834 Kwh/year, the total cost of the yearly consumption is 8722.0614 dt. Hence the profitability is calculated as follows:

$$Profitability = \frac{Cost\ of\ the\ renewable\ plant}{price\ of\ the\ yearly\ consumption} = 10.3203 years$$

6. Conclusion

An optimum sizing algorithm is proposed so as to provide the sizes of renewable generators (PVP/ Wind/ battery) supplying an autonomous agriculture farm. The sizing is based on renewable potentials, generators models and the load profile. A case study is considered in order to validate obtained results. Referring to the calculated energy balance over the year, the algorithm offers generators' sizes and water tank volume that are able to cover the farm energy need.

.

Nomenclature

E_g	Energy gap (eV)	I_{pv}	Photovoltaic generated current	v	Wind speed (ms^{-1})
$V_{t,n}$	Thermodynamic voltage (V)	V_G	Photovoltaic generated voltage	S_{wind}	Surface blades of wind turbine
I_{pv_stc}	Light-generated current at Standard Condition,	E_m	Monthly energy $(KWh/month/m^2)$	S_{ppv}	Photovoltaic panel surface
P_{cell}	Photovoltaic panel delivered power	I	Turbulence intensity	Q	Water flow $m^3.s^{-1}$
η_g	Generator efficiency	$\overline{v}$	Classified speed $(m.s^{-1})$	C	Scale factor $m.s^{-1}$
H	Height of rise (m)	S_{PPV}	Photovoltaic panel surface	P_m	Wind mean power
P_{wind}	Wind power $(W.m^{-2})$	V_{water}	Pumped water (m^3)	λ	Tip speed ratio
v_E	Energetic speed $(m.s^{-1})$	G	Irradiance on the devise surface,	C_m	Mechanical torque,
V_{water}	Pumped water (m^3)	k	Shape factor (dimensionless)	P_n	Nominal power $(W.m^{-2})$
K_1	Cell's short-circuit current temperature coefficient	P_e	Electrical power $(W.m^{-2})$	ω	Turbine angular velocity $(rad.s^{-1})$

References

Arbaoui A. (2006), Aide à la décision pour la définition d'un système éolien: Adéquation au site et à un réseau faible, Doctorate thesis, Arts And Professions Superior National School, Bordeaux center16 (Engineer'smehanical professions);.

Bashir, M., and Sadeh, J. (2012), Optimal Sizing of Hybrid Wind/Photovoltaic/Battery Considering the Uncertainty of Wind and Photovoltaic Power Using Monte Carlo, IEEE, 978-1-4577-1829-8/12.

Belfkira, R., Zhang, L., Barakat, G, (2011), Optimal sizing study of hybrid wind/PV/diesel power generation unit, Sol. Energy 85, 100–110.

Belmilin, H, Haddadi, M, Bacha, S, Almi, B. Bendib, M. (2014) Sizing stand-alone photovoltaic–wind hybrid system: Techno-economic analysis and optimization. Renewable and Sustainable EnergyReviews,30, 821–832

Brahmi, N, Chaabene, M . (2012), Sizing optimization of a wind pumping plant: Case study in Sfax, Tunisia, Journal of Renewable and Sustainable Energy 4, 013114, doi: 10.1063/1.3683530.

Cano, A, Jurado, F, Higinio Sánchez, L , Castañeda, M (2014),, optimal sizing of stand-alone hybrid systems based on pv/wt/fc by using several methodologies, Journal of the Energy Institute , Vol 87, Issue 4, pp 330–340.

Chowdhury, S.P, Chowdhury, S., Crossley, P.A. (2011). UK scenario of islanded operation of active distribution networks with renewable distributed generators, International Journal Electric Power Energy System; 33(7),1251–5.

Diaf, S., Diaf, D., Belhamel, M., Haddadi, M., and Louche, A. (2007), A methodology for optimal sizing of autonomous hybrid PV/wind system, Energy Policy, 35, 5708–5718

Eftichios, K., Dionissia, K., Antonis, P., and Kostas, K.(2006). Methodology for optimal sizing of stand-alone photovoltaic/wind-generator systems using genetic algorithms. Solar Energy, 80(9), 1072-1088.

Ekren, B.Y. and Ekren, O., (2009), Simulation based size optimization of a PV/wind hybrid energy conversion system with battery storage under various load and auxiliary energy conditions, Applied Energy, 86, 1387–1394.

Friedl, W., Schmautzer, E., Sakulin, M., Braunstein, R. (2007). Electrical energy and power saving potentials in the area Of agriculture, DUE Conference.

Glasnovic Z, and Margeta, J. (2011). Vision of total renewable electricity scenario, Renewable and Sustainable Energy; 15(4),1873–84.

Gokcek, M., Bayulken, A., Bekdemir, S. (2007), Investigation of wind characteristics and wind energy potential in Kirklareli, Turkey. Renewable Energy, 32,1739e52.

Grimsmo, L.N., Korpaas, M and Gjengeda, T (2005), Probabilistic sizing of wind and hydrogen power systems for remote areas, 15th PSCC, pp. 22-26.

Gupta, S.C., Kumar, Y.Agnihotri, G. (2007) Optimal sizing of solar-wind hybrid system, Information and Communication Technology in Electrical Sciences (ICTES), 282 - 287.

Haykin, S. (1998), Neural networks: a comprehensive foundation» Prentice-Hall, New Jersey.

Kaldellis JK, (1999), Wind energy management.Athens: Stimulus, Publications.

Kaldellis, J.K. and Zafirakis, D. (2012), Optimum sizing of stand-alone wind-photovoltaic hybrid systems for representative wind and solar potential cases of the Greek territory, Journal of Wind Engineering and Industrial Aerodynamics. 107–108, 169–178, doi.org/10.1016.

Kazem, H.A., Khatib, T., Sopian, K, (2013), Sizing of a standalone photovoltaic/battery system at minimum cost for remote housing electrification in Sohar, Oman, Energy Buildings 61, 108–115.

Lin, W.M, Hong, C.M. (2010), Intelligent approach to maximum power point tracking control strategy for variable speed wind turbine generation system., Energy, 35(6),2440–2447.

Maleki, A, Askarzadeh, A eh, (2014), Artificial bee swarm optimization for optimum sizing of a stand-alone PV/WT/FC hybrid system considering LPSP concept, Solar Energy 107, 227–235.

Maleki, A, Askarzadeh, A, (1016), Optimal sizing of a

PV/wind/diesel system with battery storage for electrification to an off-grid remote region: A case study of Rafsanjan, Iran, Journal of Sustainable Energy Technologies and Assessments.

Melício, R., Mendes, V.M.F, Catalão, J.P.S. (2011), Comparative study of power converter topologies and contr1ol strategies for the harmonic performance of variable speed wind turbine generator systems, Energy;

Musgrove, A.R.D. (1988), The optimization of hybrid energy conversion system using the dynamic programming model – RAPSODY, Int. J Energy Res. 12, 447-45.

Park, M., and Yu, I.K., (2004), A Study on Optimal Voltage for MPPT Obtained by Surface Temperature of Solar Cell, Proc. IECON, pp. 2040-2045.

Seguro, J. V. and Lambert, T. W. (2000), Estimation of the Parameters of the Weibull Wind Speed Distribution for Wind Energy Analysis. Journal of Wind Engineering and Industrial Aerodynamic.85(1), 75-84.

Silva, S. B., (2011), Sizing and Optimization Photovoltaic, Fuel Cell, IEEE Latin America Transactions, 9(1), 83-88.

Slootweg, J.G, de Haan, S.W.H., Polinder, H., Kling, W.L. (2003), General model for representing variable speed-wind turbines in power system dynamics simulations. IEEE Trans Power Syst.,18(1),144–1451.

Tina, G., Gagliano, S., Raiti, S. (2006), Hybrid solar/wind power system probabilistic modeling for long-term performance assessment, Solar Energy, 80,578-88.

Yang, H.X., Zhou, W., Lu, L., Fang, Z.H. (2008), Optimal sizing method for stand-alone hybrid solar - wind system with LPSP technology by using genetic algorithm, Solar Energy, 82(4),354-6,.

Yang, L. and Xie, M. (2003). Efficient Estimation of the Weibull Shape Parameter Based on a Modified Profile Likelihood», Journal of Statistical Computation and Simulation, 73(2), 115-123.

Yang, L., Burnett, J. H.X., (2002), Investigation on wind power potential on Hong Kong islands-an analysis of wind power and wind turbine characteristics, Renewable Energy, 27, 1-12.

Zhou, W., Lou, C., Li, Z., Lu, L., Yang, H. (2010), Current status of research on optimum sizing of stand-alone hybrid solar - wind power generation systems, Applied Energy, 87(2),380-9.